BJET
(Bayero Journal of Engineering and Technology)
https://bjet.ng/index.php/jet

Research Article
2025, Vol. 20 (1), 77-80

TOWARDS HIGH TEMPERATURE APPLICATIONS OF CARBON NANOTUBES CNTS [IV]: SPECIFIC HEAT CAPACITY OF CNTS REINFORCED SILICA NANOCOMPOSITE

Yusuf Tijjani

Department of Mechanical Engineering, Faculty of Engineering, Bayero University, Kano, Kano, Nigeria

Email: ytijjani.mec@buk.edu.ng

Received: 25-06-2025
Revised: 21-07-2025
Accepted: 27-06-2025
Published: 23-07-2025

Abstract: *Densified functionalized carbon nanotubes/silica refractory ceramic nanocomposites (FCNTs/silica) were fabricated by pressureless sintering technique. Specific heat capacity of the nanocomposites with various amounts of functionalized carbon nanotubes (FCNTs) was investigated. For the temperature range 117°C – 163°C and the different amount of FCNTs (0, 1, and 4 wt.%) were considered. The specific heat capacity isncreases with percentage FCNTs and temperature. Hence, the CNTs are outstanding reinforcement/filler for enhancing the specific heat capacity of the monolithic silica refractory ceramics.*

Key words: Silica; carbon nanotubes; silica forms; nanocomposites; specific heat capacity

1 Introduction

Silica refractory brick could be dense (≥93% SiO_2); employed in the construction of coke oven, glass furnace and hot blast stoves, lightweight (≥91% SiO_2, true porosity >45% and up to 72%); used primarily in thermal insulation of glass melting tank crowns, shaped fused or vitreous; employed as a material for hot repairs in the glass industry, and unshaped silica product (>90% SiO_2; precisely between 95 to 98%); which find application in induction furnaces for melting copper or steel (Brunk, 2001). Despite the extensive applications of silica refractory material, common setback associated with silica are brittleness and low thermal properties.

Employed as second phase inclusion/filler in silica refractory matrix; due to its exceptional mechanical and thermal properties, carbon nanotubes have been reported to improve physical and mechanical properties of the nanocomposite (Tijjani *et al.,* 2019; Tijjani *et al.,* 2018). In an attempt to address the issue of low thermal properties; specifically specific heat capacity, in natural traditional crystalline silica refractory, FCNTs have been added as a filler to the silica matrix. To the best of my knowledge, this is the first study that attempts to determine the low temperature specific heat capacity of the FCNTs/crystalline silica refractory ceramic using a pioneering pressureless sintering technique for densification.

2 Experimental Procedure

2.1 Materials

Pristine CNTs (PCNTs) (Multiwalled, CVD-grown, > 98 % purity, 10 – 20 nm diameter, and 10 – 30 µm length) were received from the Chengdu Organic Chemicals Co., Ltd, Chinese Academy of Sciences (Sichuan Sheng, China). As-mined silica/quartzite and clay both obtained from Gezawa quarry (Kano, Nigeria). CaO powder (ChemPur®, SYSTERM) was purchased from Classic Chemicals Sdn Bhd (Selangor, Malaysia).

2.2 Production of FCNTs/silica nanocomposite pellet

The silica with average particle size, $d_{(0.5)}$ = 20.166 µm, clay with size < 75 µm and CaO powder; both prepared and graded as explained by Tijjani *et al.,* 2019 were added to portion of the stable suspension of

BJET, 2025, Vol. 20 (1), 77-80

FCNTs as prepared by Tijjani *et al.,* 2018. These were thoroughly mixed, cold compacted into a pellet disk ($\emptyset 21mm \times 8mm\ height$) at 90 MPa by uni-axial hydraulic pressing machine for 2 min and dried at 150°C, for 24 h in an oven. The as-dried nanocomposite powders (FCNTs/silica) labelled 0 wt. % FCNTs + S (SC*-0), 1 wt. % FCNTs + S (SC*-1), and 4 wt. % FCNTs + S (SC*-4) were then subject to differential scanning calorimetry analysis. Where S stands for silica plus binder/mineralizer/sintering-aids (CaO + clay), C for functionalized carbon nanotubes, * means all pellet disks are unsintered and without * all pellets are sintered.

2.3 Determination of specific heat capacity of densified nanocomposite

The specific heat capacity at constant pressure (C_p) has been determined by calculation using differential scanning calorimetry (DSC), thermogravimetric/differential thermogravimetric (TG/DTG) curves obtained from TGA/DSC (1HT, Mettler Toledo) in conjunction with the **Error! R eference source not found.** below.

$$C_p = \frac{1}{m}\frac{(\delta\theta/d\tau)}{dT/d\tau} \qquad (1)$$

Where, $\delta\theta/d\tau$ is the heat flux given by the DSC curve, m is the sample mass and $(dT/d\tau) = \beta$ is the heating rate of the sample.

Typically, for the determination of C_p, thermo-analytical measurements were carried out on the unsintered FCNTs/silica powdered mixture pellets; SC*-0, SC*-1, and SC*-4 by TGA/DSC analyzer, in a dynamic air atmosphere, using respective weights of 10.1428 mg, 10.1151 mg, and 10.0158 mg in aluminium crucible 70 μL. Heating has been done at the rate of 20 K min^{-1} from room temperature (RT) to 1450°C. The necessary condition to determine the specific heat of a substance using the heat flow is that the substance must be stable in the entire temperature range which the specific heat is calculated (Morîntale *et al.,* 2013). Also, the basic assumption employed is to obtain the heat flow and eventually the specific heat capacity curves at a lower temperature corresponding to the formation of meta-stable high-temperature tridymite at 117 – 163°C occurred during the sintering of the powdered nanocomposite mixture. This same property would be applicable for the sintered FCNTs/silica refractory nanocomposite.

3 Results and Discussion

3.1 TG/DTG/DSC

Figures 1 – 3, represent the TG, DTG, and DSC curves for the SC*-0, SC*-1, and SC*-4 bricks (as-dried powders; dried at 150°C for 24 h, and then subjected to sintering process using TGA/DTG, 1HT, Mettler Toledo). In Figure 1 (with the aid of Table 1), sample SC*-0 transforms into various polymorphic phases when heated from room temperature (RT) to 1450°C in the air. It has a negligible mass loss of 0.44 %, from RT to about 116°C. Then it reversibly transformed into high-temperature metastable tridymite (β-tridymite) from low-temperature quartz (α-quartz) at 117 – 163°C. This is associated with the least volume change (0.5 %), with constant mass, and the thermal effect is zero. At approximately, 260°C, the α-quartz, reversibly transform into metastable high-temperature cristobalite (β-cristobalite) with 2 – 2.8 % volume change. Finally, the α-quartz reversibly transforms into high-temperature quartz (β-quartz). This transformation is endothermic and the β-polymorph is stable at 573 – 870°C with 0.8 – 1.3 % volume changes (precisely, the phase forms at about 618°C; Figure 1). This is the only stable polymorphic transformation that has been captured by TG, DTG, and DSC curves. There is no evidence for the formation of stable high-temperature tridymite and cristobalite modifications from β-quartz based on the TG, DTG and DSC curves. The reason may be due to the lack of impurities to facilitate the formation of β-tridymite at approximately 870°C (Heaney *et al.,* 2018). Also, for β-cristobalite, it could be due to lack of enough dwell time to precipitate-out the phase.

Similarly, for SC*-1 and SC*-4 (Figures 2 and 3 respectively, with the aid of Table 1) mass loss of 0.39 % and 0.34 % were recorded on heating the respective samples from RT to 116°C. Then, heating from 117 – 163°C resulted in an unstable reversible modification change between α-quartz and β-tridymite with constant weight and negligible volume change < 0.5 % at limiting zero thermal effect. Continuing heating to about 260°C gave rise to another metastable reversible phase β-cristobalite from α-quartz with volume change < 2 – 2.8 %. Finally, both samples transform reversibly in two steps, one exothermic; which may signify the degradation of uncoated nanotubes (at 605°C for SC*-1 and at 616°C for SC*-4) and one endothermic to a stable β-quartz polymorph from α-quartz at 654°C for SC*-1 and at 670°C for SC*-4. This transformation is observable from TG, DTG, and DSC curves as is the only stable polymorphic change. Other modification changes such as the formation of stable β-tridymite and β-cristobalite were not detected in the curves. The reason may be lack of enough transformation periods.

BJET, 2025, Vol. 20 (1), 77-80

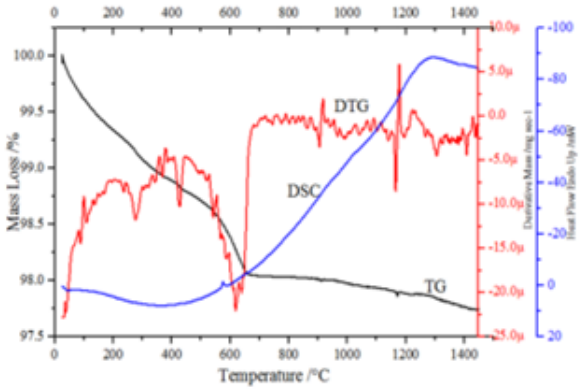

Figure 1: Thermo-analytical curves of SC-0 in air*

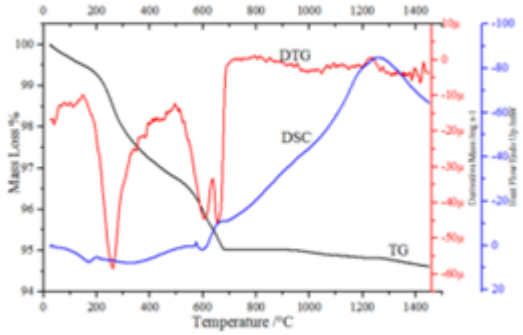

Figure 2: Thermo-analytical curves of SC-1*

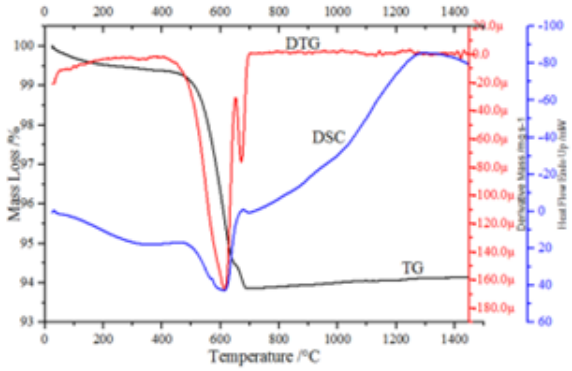

Figure 3: Thermo-analytical curves of SC-4 in air*

Table 1: Modification and volume changes of Silica

Modification Changes reversible ↔ irreversible →	Transformation Temperature [°C]	Volume Change [%]
α ↔ β-quartz	573	0.8 – 1.3
β-quartz → β-cristobalite	1250 (~ 1050 #)	17.4
α ↔ β-cristobalite	~ 260	2 – 2.8
β-quartz → β-tridymite #	~ 870	14.4
γ ↔ α ↔ β-tridymite #	117- 163	0.5
β-tridymite → β-cristobalite	1470	0

In presence of impurities, source: (Almarahle, 2005; Brunk, 2001).

Where:

α- is the low-temperature modification of quartz, tridymite, and cristobalite; β- is the high-temperature modification of quartz, tridymite, and cristobalite.

3.2 Specific Heat Capacity of FCNTs/silica

For the determination of specific heat capacity, the areas of mass stability and absence of heating effects are usually selected. From Figures 1 – 3, these areas are identified to be the temperature range for the formation of metastable high-temperature tridymite 117 – 163°C. Consistent with the previous studies (Morîntale *et al.,* 2013; Degeratu *et al.,* 2013; Degeratu *et al.,* 2009; Harabor *et al.,* 2013), heat flow from the DSC curves in conjunction with equation 1, is applied to evaluate the specific heat capacities of FCNTs/silica nanocomposites in the air and are depicted in Figure 4.

The C_p values are found to increase with temperature and with percentage FCNTs under the measured temperature range. This trend coincided well with the results of the previous studies. For instance, it was reported that the C_p values increased with increased temperature as well as the proportion of MWNTs in MWNT-TiN composites (Jiang & Gao, 2008). They attributed the increased to the contribution of MWNTs in the composites. The same reasons have been mentioned in the case of CNT – $BaTiO_3$ (Huang *et al.,* 2005).

BJET, 2025, Vol. 20 (1), 77-80

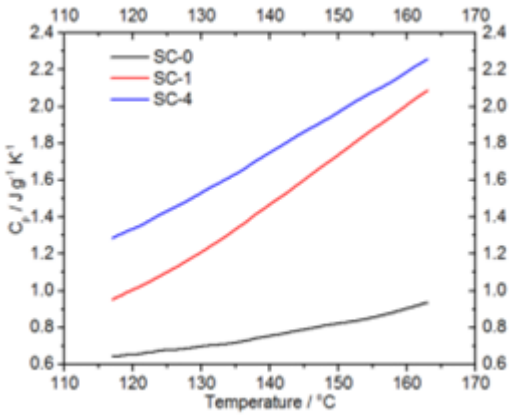

Figure 4: *The specific heat capacity of FCNTs/silica bricks*

4 Conclusion

The specific heat capacity at constant pressure (Cp) of FCNTs/silica nanocomposites as obtained using heat flow from the DSC curves and equation 1 has been found to increase with temperature and % CNTs. Overall, this article demonstrates the potential of FCNTs/silica nanocomposites to improve the thermal properties of refractory materials, enabling new applications and improving efficiency and durability in various industries such as aerospace, defense, and energy.

References

Almarahle, G., 2005. Production of silica-refractory bricks from white sand. *American Journal of Applied Sciences*, *2*(1), pp.465-468.

Brunk, F., 2001. Silica refractories. *CN Refractories(Germany)*, *5*, pp.27-30.

Degeratu, S., Rotaru, P., Rizescu, S. and Bîzdoacă, N.G., 2013. Thermal study of a shape memory alloy (SMA) spring actuator designed to insure the motion of a barrier structure. *Journal of thermal analysis and calorimetry*, *111*(2), pp.1255-1262.

Degeratu, S., Rotaru, P., Manolea, G., Manolea, H. and Rotaru, A., 2009. Thermal characteristics of Ni–Ti SMA (shape memory alloy) actuators. *Journal of thermal analysis and calorimetry*, *97*(2), pp.695-700.

Harabor, A., Rotaru, P. and Harabor, N.A., 2013. Thermal and spectral behavior of (Y, Eu) VO4 powder. *Journal of thermal analysis and calorimetry*, *111*(2), pp.1211-1219.

Heaney, P.J., Prewitt, C.T. and Gibbs, G.V. eds., 2018. *Silica: Physical behavior, geochemistry, and materials applications* (Vol. 29). Walter de Gruyter GmbH & Co KG.

Huang, Q., Gao, L., Liu, Y. and Sun, J., 2005. Sintering and thermal properties of multiwalled carbon nanotube–BaTiO 3 composites. *Journal of Materials Chemistry*, *15*(20), pp.1995-2001.

Jiang, L. and Gao, L., 2008. Densified multiwalled carbon nanotubes–titanium nitride composites with enhanced thermal properties. *Ceramics international*, *34*(1), pp.231-235.

Liu, D.M., Tuan, W.H. and Chiu, C.C., 1995. Thermal diffusivity, heat capacity and thermal conductivity in Al2O3□ Ni composite. *Materials Science and Engineering: B*, *31*(3), pp.287-291.

Morîntale, E., Harabor, A., Constantinescu, C. and Rotaru, P., 2013. Use of heat flows from DSC curve for calculation of specific heat of the solid materials. *Physics AUC*, *23*, pp.89-94.

TIJJANI, Y., YASIN, F. M., ISMAIL, M. H. S., and ARIFF, A. H. M., 2018. Manufacturing and mechanical characterization of multiwalled carbon nanotubes/quartz nanocomposite. *Journal of the Ceramic Society of Japan, 126 (12),* pp.984-991.

Tijjani, Y., Yasin, F. M., Ismail, M. H. S., & Hanim, M. A., 2019. Effect of Carbon nanotubes addition on the foundry physical properties of Silica refractory nanocomposite: PART A. *In IOP Conference Series: Materials Science and Engineering* (Vol. 469, No. 1, pp. 012022). IOP Publishing.